Analyzing Potential Improvements to a Semi-Analytical CO_2 Leakage Algorithm

Brent Cody[1], Ana González-Nicolás, Domenico Baù

Department of Civil and Environmental Engineering, Colorado State University

Abstract. A long history of using of fossil fuels has resulted in increased atmospheric CO_2 concentrations. This anthropogenic process has influenced global climate change. One possible way to retard this increasing atmospheric concentration is to geologically sequester CO_2 emissions. Successfully implementation of this technology requires a full understand of associated risks and detailed resource optimization. It is important to choose the appropriate level of complexity when selecting the type of simulation model to apply to this problem. Many risk assessment and optimization tools require large numbers of realizations. In most cases, using a full scale numerical CO_2 leakage model for this process becomes computationally prohibitive. Therefore, faster CO_2 leakage estimations are needed. An excellent semi-analytical multi-phase CO_2 leakage algorithm has been developed by Celia et al. (2011). In the following work, three possible accuracy improvements to this algorithm are proposed and explored. Differences between leakage rates and pressure distributions are compared between existing and modified methods. Improvement suggestions are then made from these observations.

Introduction

Preliminary stages of geological storage (GS) site selection, optimization, and sensitivity analysis require large numbers of model simulations. It is often beneficial to use faster, though less accurate, leakage estimation models for 'coarse' scale project development. After narrowing down the set of possible solutions, more sophisticated, although slower, numerical models should be used for detailed project development.

A semi-analytical algorithm, developed by Celia et. al. (2011) and Nordbotten et. al. (2009), estimates both brine and CO_2 flux through permeable caprock locations caused by GS. Originally conceptualized as segments of abandoned wells, permeable caprock locations represent cylindrical portions of the aquitard layers having permeability values greater than or equal to zero. Referred to as 'leaky wells', these are the only pathways for fluid flux between aquifer layers.. Users of this model are able to specify the number and spatial location of injection wells (M), leaky wells (N), and aquifer/aquitard layers (L).

The domain is structured as a horizontal stack of aquifer/aquitard layers perforated by injection and leaky wells. Aquifers are assumed to be horizontally level, homogenous, and isotropic. Aquitards are impermeable, except where perforated by leaky wells. Injection wells are able to inject into any layer.

---

[1] Groundwater Hydrology Division
Civil Engineering Department
Colorado State University
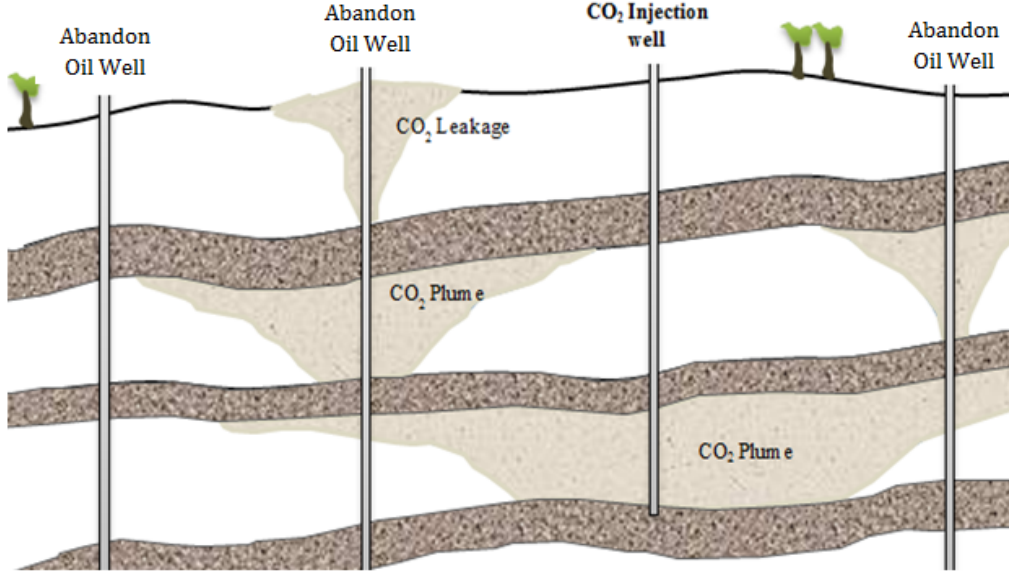Fort Collins, CO 80523-1372
e-mail: codybm@engr.colostate.edu

Figure 1. Domain Schematic

Initially, fluid is not flowing through any of the leaky wells because the entire domain is assumed to be saturated with brine at hydrostatic pressure. At the start of fluid injection the pressure throughout the domain begins to change resulting in fluid flux through leaky wells. It is therefore very important to understand aquifer fluid pressure responses regarding changes in CO_2 and brine storage volumes. Celia et. al. (2011) presents the pressure distribution in a confined aquifer for a single well injecting CO_2 as

$$
\Delta p'(\chi) - F(h')
$$
$$
= \begin{cases}
0, & \chi \geq \psi \\
-\dfrac{1}{2\Gamma} \ln\left(\dfrac{\chi}{\psi}\right) + \Delta p'(\psi), & \psi > \chi \geq 2\lambda \\
\dfrac{1}{\Gamma} - \dfrac{\sqrt{\chi}}{\Gamma\sqrt{2\lambda}} + \Delta p'(2\lambda), & 2\lambda > \chi \geq \dfrac{2}{\lambda} \\
-\dfrac{1}{2\lambda\Gamma} \ln\left(\dfrac{\chi\lambda}{2}\right) + \Delta p'\left(\dfrac{2}{\lambda}\right) - F(h'), & \dfrac{2}{\lambda} > \chi
\end{cases} \tag{1}
$$

where

$$
\chi = \frac{2\pi H\varphi(1 - S_b^{res})r^2}{Q_{well}t} \tag{2}
$$

$$
\Gamma = \frac{2\pi(\rho_B - \rho_C)gkH^2}{\mu_b Q_{well}} \tag{3}
$$

$$
\psi = \frac{4.5\pi H\varphi k(1 - S_b^{res})r^2}{\mu_b c_{eff} Q_{well}} \tag{4}
$$

$$\Delta p' = \frac{p - p_0}{(\rho_b - \rho_c)gH} \tag{5}$$

$$h' = \frac{h(\chi)}{H} = \frac{1}{\lambda - 1}\left(\frac{\sqrt{2\lambda}}{\sqrt{\chi}} - 1\right) \tag{6}$$

$$F(h') = \frac{-\lambda}{\lambda - 1}\left[h' - \frac{ln[(\lambda - 1)h' + 1]}{\lambda - 1}\right] \tag{7}$$

In (1-7), subscripts b and c denote brine and CO_2, respectively, λ refers to total aquifer mobility. B, H, and h are aquitard, aquifer, and CO_2 plume thicknesses, respectively. S_b^{res} is the residual saturation of the brine, t is injection duration, k is permeability, c_{eff} is the effective compressibility of the aquifer, g is gravitational acceleration, μ is dynamic viscosity, φ is porosity, r is radial distance, ρ is fluid density, and Q_{well} is the total volumetric well flux. $F(h')$ is an offset term resulting from solving the ordinary differential pressure equation (17) in Nordbotten and Celia (2006).

The semi-analytical algorithm uses (1) to determine the pressure distribution throughout the aquifer then applies the multiphase version of Darcy's law to determine leaky well flow rates.

$$Q_{\alpha,well,l} = \pi r_{pw}{}^2_{well,l}\frac{k_{r,\alpha}k_{well,l}}{\mu_\alpha B_l}\left(p_{well,l-1} - \rho_b g B_l - g\rho_b H_{l-1} - p_{well,l}\right) \tag{8}$$

In (8) k_r is relative conductivity and α denotes phase type (either c for CO_2 or b for brine).

Unlike the Theis Equation, (1) is both non-linear and discontinuous. Also, unlike single phase flow, CO_2 plume locations and thicknesses must be known when determining fluid saturations and relative permeabilities found in leaky well pathways.

These problems are overcome by linearizing the pressure equation using Green's functions and applying time-stepping to approximate the changing pressure distribution, CO_2 plume locations and thicknesses, and leaky well fluxes over the injection duration.

For each time-step, the following linear equation is written for each leaky well at the bottom of each aquifer.

$$p_{w,l} = p_{int,l} + \sum_{well=1}^{M} G_{w,l,well}Q_{well,l}$$
$$+ \sum_{well=M+1}^{M+N} G_{w,l,well}\{Q_{well,l} - Q_{well,l+1}\} + F(h'_{max}) \tag{9}$$

In (9) p is the fluid pressure at the bottom of the aquifer, w denotes the well at which pressure is being solved, l denotes the aquifer layer, *well* denotes the well flux adding or subtracting pressure at well w. Also,

$$G_{w,l,well} = \frac{\partial p_{w,l}}{\partial Q_{well,l}} \tag{10}$$

Nordbotten et. al. (2009) describes these Green's functions as representations of "the sensitivity of the pressure field for a given source or sink". They are found by calculating the partial derivative of (1) with respect to Q_{well}. For each time-step, Green's functions are evaluated using start of time-step flow rates. This results in $G_{w,l,well}$ being a constant value for each time-step.
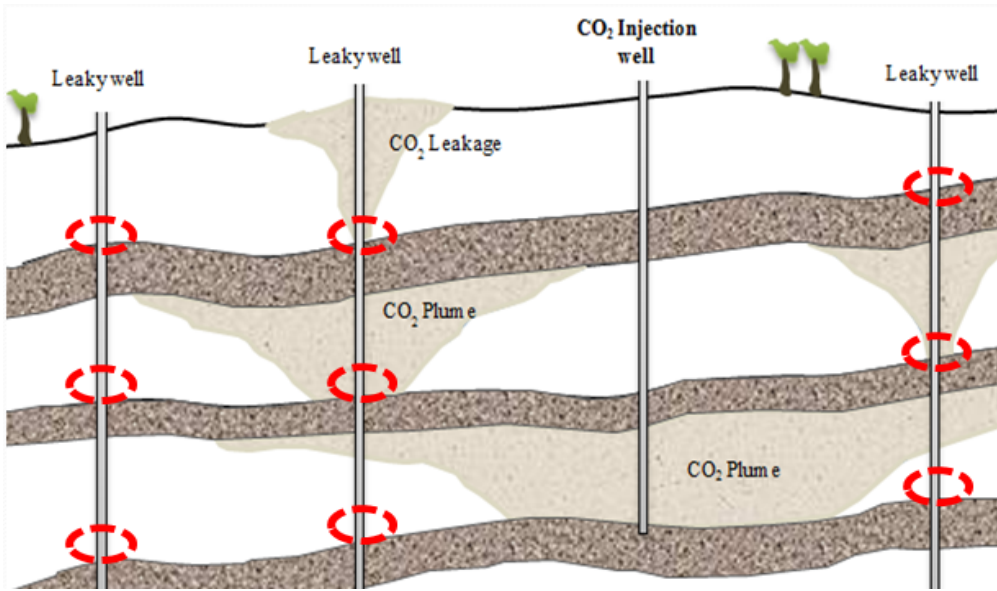

Figure 2. Pressure unknowns for this domain are located at the red circles

Substituting (8) into (9) yields the following,

$$
\begin{aligned}
p_{w,l} &= p_{int,l} + \sum_{well=1}^{M} G_{w,l,well} Q_{well,l} \\
&+ \sum_{well=M+1}^{M+N} G_{w,l,well} \left\{ \pi r_{pw}^2{}_{well,l} k_{well,l} \frac{k_{r,eff,well,l}}{\mu_{eff} B_l} \left(p_{well,l-1} - \rho_b g B_l \right. \right. \\
&\quad \left. - gH_{l-1}(\rho_b - \rho_b h'_{w,l-1} + \rho_c h'_{w,l-1}) - p_{well,l} \right) \\
&\quad - \pi r_{pw}^2{}_{well,l+1} k_{well,l+1} \frac{k_{r,eff,well,l+1}}{\mu_{eff} B_{l+1}} \left(p_{well,l} - \rho_b g B_{l+1} \right. \\
&\quad \left. \left. - gH_l(\rho_b - \rho_b h'_{w,l} + \rho_c h'_{w,l}) - p_{well,l+1} \right) \right\} + F(h'_{max})
\end{aligned}
\tag{11}
$$

where the subscript *eff* denotes 'effective'. Effective phase dependent parameters are needed because Q_{well} may be composed of both CO$_2$ and brine. It is now possible to isolate the unknown pressure terms $p_{w,l}$, $p_{well,l-1}$, $p_{well,l}$, and $p_{well,l+1}$.

$$
\begin{aligned}
p_{w,l} & \\
+ \sum_{well=M+1}^{M+N} & \left\{ \left[-G_{w,l,well}\pi r_{pw}^2{}_{well,l} k_{well,l} \frac{k_{r,eff,well,l}}{\mu_{eff}B_l} \right] p_{well,l-1} \right. \\
& + \left[G_{w,l,well}\pi r_{pw}^2{}_{well,l} k_{well,l} \frac{k_{r,eff,well,l}}{\mu_{eff}B_l} \right. \\
& + G_{w,l,well}\pi r_{pw}^2{}_{well,l+1} k_{well,l+1} \frac{k_{r,eff,well,l+1}}{\mu_{eff}B_{l+1}} \left. \right] p_{well,l} \\
& + \left. \left[-G_{w,l,well}\pi r_{pw}^2{}_{well,l+1} k_{well,l+1} \frac{k_{r,eff,well,l+1}}{\mu_{eff}B_{l+1}} \right] p_{well,l+1} \right\} \\
= p_{int,l} & + \sum_{well=1}^{M} \left[G_{w,l,well}Q_{well,l} \right] \\
+ \sum_{well=M+1}^{M+N} & \left[G_{w,l,well} \left\{ \pi r_{pw}^2{}_{well,l} k_{well,l} \frac{k_{r,eff,well,l}}{\mu_{eff}B_l}(-\rho_b g B_l \right.\right. \\
& - gH_{l-1}(\rho_b - \rho_b h'_{w,l-1} + \rho_c h'_{w,l-1})) \\
& - \pi r_{pw}^2{}_{well,l+1} k_{well,l+1} \frac{k_{r,eff,well,l+1}}{\mu_{eff}B_{l+1}}(-\rho_b g B_{l+1} \\
& \left.\left. - gH_l\left(\rho_b - \rho_b h'_{w,l} + \rho_c h'_{w,l}\right)) \right\} \right] + F(h'_{max})
\end{aligned} \tag{12}
$$

(12) can be written as

$$
p_{w,l} + \sum_{well=M+1}^{M+N} \left(A_{w,l,well}p_{well,l-1} + B_{w,l,well}p_{well,l} + C_{w,l,well}p_{well,l+1} \right) \\
= D_{w,l} \tag{13}
$$

where A, B, C, and D are constants for the current time-step. The set of linear equations in matrix form for a domain having 3 aquifer/aquitard layers and 2 leaky wells would be written as

$$
\begin{bmatrix}
B_{1,1,1}+1 & B_{1,1,2} & C_{1,1,1} & C_{1,1,2} & 0 & 0 \\
B_{2,1,1} & B_{2,1,2}+1 & C_{2,1,1} & C_{2,1,2} & 0 & 0 \\
A_{1,2,1} & A_{1,2,2} & B_{1,2,1}+1 & B_{1,2,2} & C_{1,2,1} & C_{1,2,2} \\
A_{2,2,1} & A_{2,2,2} & B_{2,2,1} & B_{2,2,2}+1 & C_{2,2,1} & C_{2,2,2} \\
0 & 0 & A_{1,3,1} & A_{1,3,2} & B_{1,3,1}+1 & B_{1,3,2} \\
0 & 0 & A_{2,3,1} & A_{2,3,2} & B_{2,3,1} & B_{2,3,2}+1
\end{bmatrix}
\begin{bmatrix}
p_{1,1} \\ p_{2,1} \\ p_{1,2} \\ p_{2,2} \\ p_{1,3} \\ p_{2,3}
\end{bmatrix}
=
\begin{bmatrix}
D_{1,1} \\ D_{2,1} \\ D_{1,2} \\ D_{2,2} \\ D_{1,3} \\ D_{2,3}
\end{bmatrix}
\tag{14}
$$

Solving (14) provides end of time-step pressures at each leaky well at each layer. It is now possible to calculate end of time-step leaky well segment fluxes using (8). The time-step is then advanced and the process is repeated until the injection duration is reached.

CO_2 and brine volumetric storage changes in each layer, $\Delta V_{\alpha,l}$, can then be determined by multiplying the injection duration, t_{inj}, by the sum of average leaky well segment flow rates, $Q_{\alpha,avg}$.

$$\Delta V_{\alpha,l} = t_{inj} \sum_{well=1}^{M+N} \left[Q_{\alpha,avg,well,l} - Q_{\alpha,avg,well,l+1} \right] \tag{15}$$

Accuracy Improvement Testing

The following discussion analyzes possible accuracy improvements to this algorithm. Three possible accuracy improvements have been tested and are described below. Due to the complexity of the underlying concepts we have attempted to keep the simulation domains as simple as possible. Improvement testing involved: 1) looking at the radial pressure distribution for a single injection well injecting into a single confined aquifer without any leaky wells, and/or 2) comparing flow rates and fluid pressures at a single leaky well in a domain having 2 aquifer layers and 1 injection well.

Unless otherwise specified each simulation had the following parameters: an injection duration of 2500 days, aquifer and aquitard thicknesses of 15m, an injection rate of 50 kg/s of CO_2, $\lambda = 5$, $S_b^{res} = 5\%$, an aquifer permeability of 1 mD, a leaky well permeability = 100 mD, $c_{eff} = 4.6$ x 10^{-10} m^2/N, $g = 9.81$ m/s^2, $\rho_b = 1000$ kg/m^3, $\rho_c = 600$ kg/m^3, $\mu_b = 0.5$ mPa s, $\mu_c = 0.05$ mPa s, and a horizontal distance between the injection well and the leaky well of 1 km.

__Significance of F(h)__

The existing work makes the assumption that only the offset term having the maximum absolute value, $F(h'_{max})$, is relevant when superimposing pressure change effects using (9). This section explores the suggestion of including each well's offset term when superimposing pressure changes. Applying this modification would change (9) into

$$p_{w,l} = p_{int,l} + \sum_{well=1}^{M} \left[G_{w,l,well} Q_{well,l} + F(h'_{w,l,well}) \right]$$
$$+ \sum_{well=M+1}^{M+N} \left[G_{w,l,well} \{ Q_{well,l} - Q_{well,l+1} \} \right. \tag{16}$$
$$\left. + F(h'_{w,l,well}) \right]$$

As seen in (7), $F(h')$ is dependent upon only λ and h'. Aquifer fluid pressure changes resulting from this offset term, Δp_F, are calculated using

$$\Delta p_F = F(h')(\rho_B - \rho_C)gH \tag{17}$$

The absolute values of both $F(h')$ and Δp_F are greatest when $h'=1$ (i.e. when the CO_2 plume thickness is equal to the aquifer thickness). Figure 3 shows the pressure changes resulting from $F(h'=1)$ verses aquifer mobility for our set of simulation parameters listed above.
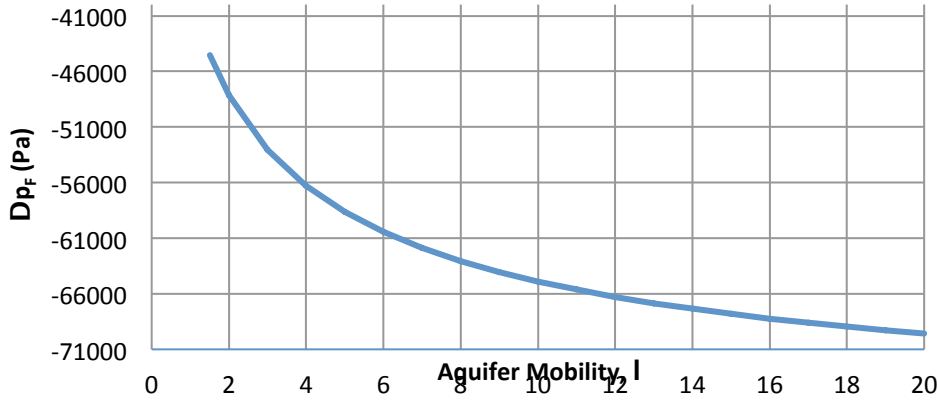

Figure 3. Pressure change resulting from *F(h'=1)* vs. λ

As seen in Figure 3, Δp_F is always negative and is therefore a pressure reduction term. When domains have thick or highly permeable aquifers this term greatly reduces near well fluid pressures. Figure 4 shows aquifer pressure increases verses radial distance with an aquifer thickness of 60 m.
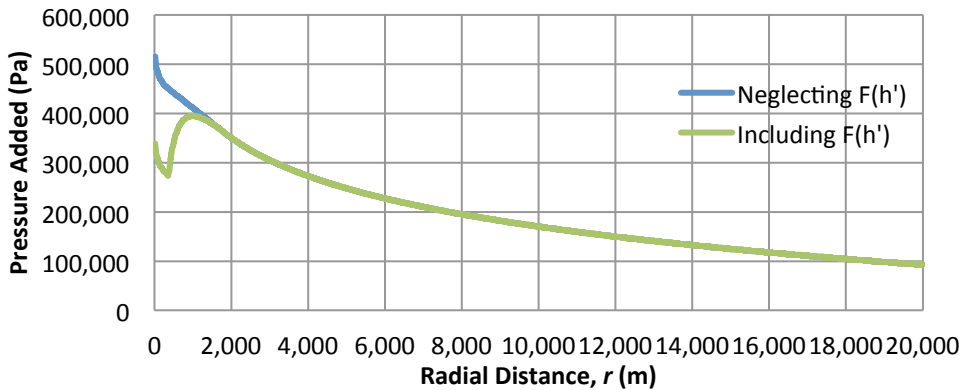

Figure 4. Pressure change vs. radial distance for CO_2 injection into a 60m thick aquifer

Certain conditions assumed when deriving (1) in Nordbotten and Celia (2006) were violated to produce the infeasible solution shown in Figure 4. The analytical solution was derived for Γ being negligibly small. As seen in Equation (3), Γ increases quadraticly with increasing aquifer thickness.

Figure 5 shows aquifer pressure increases verses radial distance with an aquifer thickness of 15 m. When the domain has relatively low aquifer permeabilities and thicknesses (1)'s assumed conditions are met and $F(h')$ is negligible. This suggests that

when applying this model first check if $F(h')$ is negligible. If this is not the case, the injection site's domain is not suitable for this analytical solution.
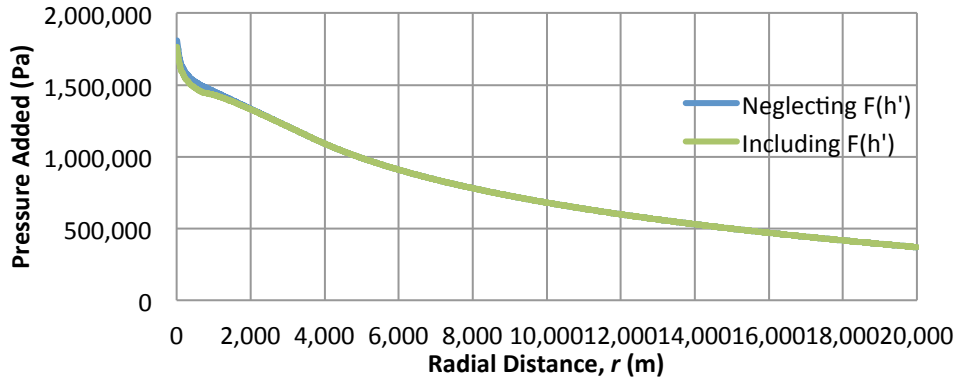

Figure 5. Pressure change vs. radial distance for CO_2 injection into a 15m thick aquifer

Use of Average Flow Rates

The CO_2 pressure equation (1) was derived with the assumption that Q_{well} is a constant CO_2 flux. We can approximate effects from a changing flux by using an average. The existing algorithm uses end of time-step leaky flow rates, $Q_{well,t}$, when writing the set of linear equations (9). This technique will herein be referred to as the "End of Time-step Flux Solver" (ETS) method.

Figure 6 shows an example of a leaky well's flux (represented by the blue line) increasing with time. Multiplying $Q_{well,t}$ (represented by the orange line) by t overestimates the volume of fluid transferred by a source if $Q_{well,t}$ is greater than $Q_{well,avg,t}$ (represented by the green line).
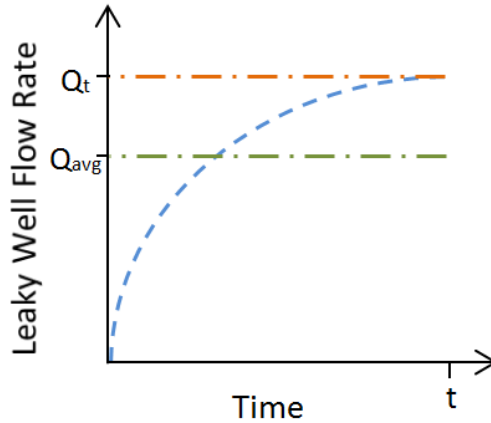

Figure 6. Leaky well flow rate vs. time

The set of linear equations should be written with respect to $Q_{well,avg}$.

$$
\begin{aligned}
p_{w,l} = p_{int,l} &+ \sum_{well=1}^{M} G_{w,l,well} Q_{well,avg,l} \\
&+ \sum_{well=M+1}^{M+N} G_{w,l,well} \{Q_{well,avg,l} - Q_{well,avg,l+1}\}
\end{aligned}
\tag{18}
$$

The average volumetric flow rate equals the total fluid mass transferred by the leaky well segment, $M_{well,l}^t$, divided by the effective fluid density, ρ_{eff}, divided by the time, t.

$$Q_{well,avg,l}^t = M_{well,l}^t / \rho_{eff} t \tag{19}$$

Effective densities are needed because $M_{well,l}^t$ may be composed of both CO$_2$ and brine. The total fluid mass transferred by the leaky well segment at the end of the time-step can be calculated by

$$M_{well,l}^t = M_{well,l}^{t-\Delta t} + 0.5\Delta t \left(Q_{well,,l}^{t-\Delta t} + Q_{well,l}^t\right)\rho_{eff} \tag{20}$$

where Δt is time-step duration. Substituting (20) into (19) gives

$$Q_{well,avg,l}^t = \left[M_{well}^{t-\Delta t,l} + 0.5\Delta t \left(Q_{well}^{t-\Delta t,l} + Q_{well}^{t,l}\right)\rho_{eff}\right]/\rho_{eff} t \tag{21}$$

Subtracting the bottom by the top layer average flow rates gives

$$\begin{aligned}
Q_{well,avg,l} &- Q_{well,avg,l+1} \\
&= \big[M_{well}^{t-\Delta t,l} - M_{well}^{t-\Delta t,l+1} \\
&\quad + 0.5\Delta t\{\left(Q_{well}^{t-\Delta t,l} + Q_{well}^{t,l}\right) \\
&\quad - \left(Q_{well}^{t-\Delta t,l+1} + Q_{well}^{t,l+1}\right)\}\rho_{eff}\big]/\rho_{eff} t
\end{aligned} \tag{22}$$

Time-step constants c_c and c_2 are defined as,

$$c_c = \frac{M_{well}^{t-\Delta t,l} - M_{well}^{t-\Delta t,l+1} + 0.5\Delta t \left(Q_{well}^{t-\Delta t,l} - Q_{well}^{t-\Delta t,l+1}\right)\rho_{eff}}{\rho_{eff} t} \tag{23}$$

$$c_2 = \frac{0.5\Delta t}{t} \tag{24}$$

Using c_c and c_2, (22) can be written concisely as

$$Q_{well,avg,l} - Q_{well,avg,l+1} = c_2\left(Q_{well,l} - Q_{well,l+1}\right) + c_c \tag{25}$$

Substituting (25) into (18) gives the modified pressure equation for the "Average Flux Solver" (AS) method.

$$p_{w,l}$$

$$= p_{int,l} + \sum_{well=1}^{M} \left[G_{w,l,well} Q_{well,l} \right]$$

$$+ \sum_{well=M+1}^{M+N} \left[c_2 G_{w,l,well} \left\{ \pi r_{pw_{well,l}}^2 k_{well,l} \frac{k_{r,eff,well,l}}{\mu_{eff} B_l} (p_{well,l-1} \right. \right.$$

$$- \rho_b g B_l - g H_{l-1} (\rho_b - \rho_b h'_{w,l-1} + \rho_c h'_{w,l-1}) - p_{well,l})$$

$$- \pi r_{pw_{well,l+1}}^2 k_{well,l+1} \frac{k_{r,eff,well,l+1}}{\mu_{eff} B_{l+1}} (p_{well,l} - \rho_b g B_{l+1} - g H_l (\rho_b$$

$$\left. \left. - \rho_b h'_{w,l} + \rho_c h'_{w,l}) - p_{well,l+1}) \right\} + c_c G_{w,l,well} \right]$$

(26)

Figure 7 compares CO_2 and brine leaky well flux rates verse time calculated using the ETS and AS methods. In this case, leaky well CO_2 flux is estimated to be greater when using the AS method. Recall from (10) that $\Delta p = G*Q$. If Q_t is greater than Q_{avg}, the change in pressure calculated by $G*Q_t$ will be greater than the change is pressure calculated by $G*Q_{avg}$. As a result, artificially low leaky well flow rates are estimated when $Q_t > Q_{avg}$ and the ETS method ($G*Q_t$) is used to estimate pressure changes.
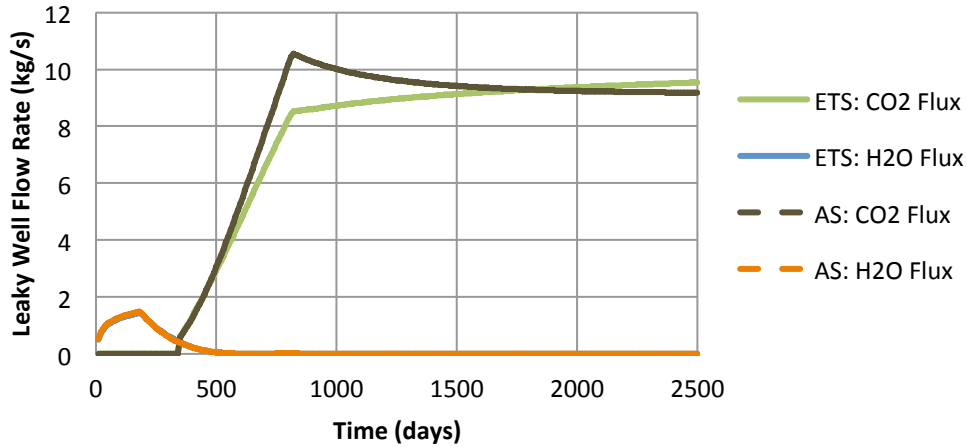

Figure 7. Leaky well flow rates vs. time

It is also important to note that in Figure 7 the steep increase in CO_2 flux rates (t = ~400 - 800 days) occurs as a result of the rapidly increasing CO_2 relative permeability in the leaky well due to the increasing plume thickness. The slope of CO_2 flux vs. time abruptly lessens around t = 800 days when the CO_2 relative permeability reaches unity (k_{rc} = 1) and is unable to continue increasing.

Aquifer fluid pressures at the leaky well determined using the ETS and AS methods are compared in Figure 8. Intuitively, pressures determined by the AS method seem correct. The blue dashed line shows pressure in the lower aquifer building rapidly in the first 500 days then reaching a semi steady-state condition. The green dashed line shows

pressure in the top aquifer remaining low until sufficient pressure builds up in the bottom aquifer and the relative conductivity of CO_2 in the leaky well approaches unity. As seen in Figure 7, the leaky well flux reaches a maximum once these conditions are met because of a build-up of pressure in the lower aquifer caused by earlier low relative conductivities. The leaky well flow rate begins to subside as the fluid pressure begins to increase in the top aquifer, reducing the pressure gradient across the aquitard.
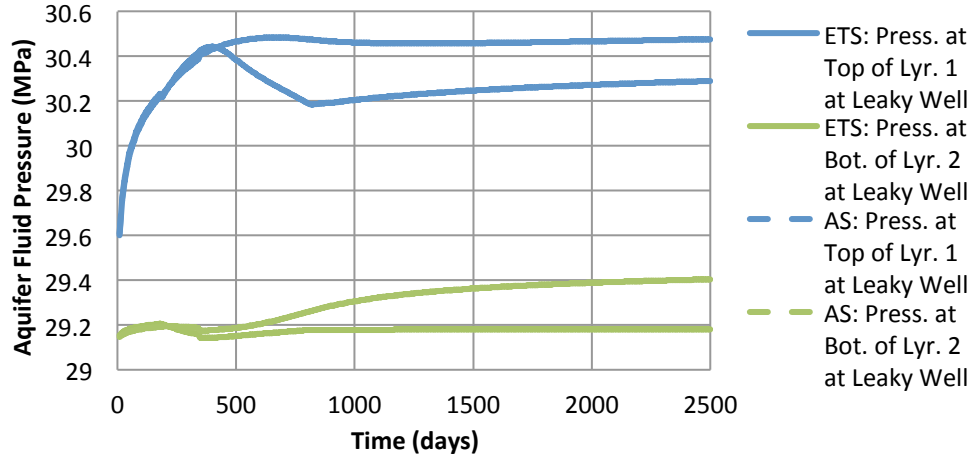

Figure 8. Aquifer fluid pressures vs. time

Figure 8 also shows that aquifer fluid pressures are found to have less abrupt transitions through time when using the AS method. This is because the AS method directly accounts for the flow rate history when calculating end of time-step flow rates.

This analysis suggests that the AS method should always be used with applying this algorithm. The AS method multiplies the correct flow rate by the Green's functions, gives smoother fluid pressure verse time profiles, and therefore provides a more accurate leakage estimation.

CO₂ and Brine Separation

The existing algorithm takes the sum of the CO_2 and brine flow rates to calculate the total volumetric source or sink when determining Q_{well} for the pressure equation. This technique will be referred to as the "Combined Flux" (CF) method. A "Separated Flux" (SF) method may improve this algorithm by eliminating the need to make assumptions concerning the discontinuous nature of (1) and effective phase dependent parameters, such as density, relative conductivity.

The SF method uses (1) to determine pressure added from CO_2 leakage and the Theis Equation,

$$p_{w,l} - p_{int,l} = \frac{\rho_b g}{4\pi T_l} W(u_{w,l,well}) Q_{b,l} \tag{27}$$

where,

$$u_{w,l,well} = \frac{r_{w,well}^2 S_l}{4 T_l t} \tag{28}$$

to determine pressure added from brine leakage. In (27) and (28) T_l is the layer transmissivity, $W(u)$ is the Well function, $r_{w,well}$ is the horizontal distance between well 'w' and well '$well$', and S_l is the layer storativity. The SF method modifies the superpositioning of pressure sources as follows:

$$
\begin{aligned}
p_{w,l} = p_{int,l} &+ \sum_{well=1}^{M} \left[G_{w,l,well} Q_{c,well,l} + \frac{\rho_b g}{4\pi T_l} W(u_{w,l,well}) Q_{b,well,l} \right] \\
&+ \sum_{well=M+1}^{M+N} \left[G_{w,l,well} \{ Q_{c,well,l} - Q_{c,well,l+1} \} \right] \\
&+ \frac{\rho_b g}{4\pi T_l} \sum_{well=M+1}^{M+N} \left[W(u_{w,l,well}) \{ Q_{b,well,l} - Q_{b,well,l+1} \} \right]
\end{aligned}
\tag{29}
$$

The definition of c_c must be redefined and a similar term for brine, c_b, must be created to apply the AS method to the SF method.

$$
c_c = \frac{M_c^{t-\Delta t,l} - M_c^{t-\Delta t,l+1} + 0.5\Delta t \left(Q_c^{t-\Delta t,l} - Q_c^{t-\Delta t,l+1} \right)}{\rho_c t}
\tag{30}
$$

$$
c_b = \frac{M_b^{t-\Delta t,l} - M_b^{t-\Delta t,l+1} + 0.5\Delta t \left(Q_b^{t-\Delta t,l} - Q_b^{t-\Delta t,l+1} \right)}{\rho_b t}
\tag{31}
$$

$$
\begin{aligned}
p_{w,l} = p_{int,l} &+ \sum_{well=1}^{M} \left[G_{w,l,well} Q_{c,well,l} + \frac{\rho_b g}{4\pi T_l} W(u_{w,l,well}) Q_{b,well,l} \right] \\
&+ \sum_{well=M+1}^{M+N} \left[c_2 G_{w,l,well} \{ Q_{c,well,l} - Q_{c,well,l+1} \} \right. \\
&\qquad\qquad \left. + c_c G_{w,l,well} \right] \\
&+ \frac{\rho_b g}{4\pi T_l} \sum_{well=M+1}^{M+N} \left[c_2 W(u_{w,l,well}) \{ Q_{b,well,l} - Q_{b,well,l+1} \} \right. \\
&\qquad\qquad \left. + c_b W(u_{w,l,well}) \right]
\end{aligned}
\tag{32}
$$

Substituting (8) into (31) gives

$$p_{w,l}$$

$$= p_{int,l} + \sum_{well=1}^{M} \left[G_{w,l,well} Q_{c,l} + \frac{\rho_b g}{4\pi T_l} W(u_{w,l,well}) Q_{b,l} \right]$$

$$+ \sum_{well=M+1}^{M+N} \left[c_2 G_{w,l,well} \left\{ \pi r_{pw}^2{}_{well,l} k_{well,l} \frac{k_{rc\,well,l}}{\mu_c B_l} (p_{well,l-1} - \rho_b g B_l \right. \right.$$

$$- gH_{l-1}(\rho_b - \rho_b h'_{w,l-1} + \rho_c h'_{w,l-1}) - p_{well,l})$$

$$- \pi r_{pw}^2{}_{well,l+1} k_{well,l+1} \frac{k_{rc\,well,l+1}}{\mu_c B_{l+1}} (p_{well,l} - \rho_b g B_{l+1} - gH_l(\rho_b$$

$$- \rho_b h'_{w,l} + \rho_c h'_{w,l}) - p_{well,l+1}) \Big\} + c_c G_{w,l,well} \bigg]$$

$$+ \frac{\rho_b g}{4\pi T_l} \sum_{well=M+1}^{M+N} \left[c_2 W(u_{w,l,well}) \left\{ \pi r_{pw}^2{}_{well,l} k_{well,l} \frac{k_{rb\,well,l}}{\mu_b B_l} (p_{well,l-1} \right. \right.$$

$$- \rho_b g B_l - gH_{l-1}(\rho_b - \rho_b h'_{w,l-1} + \rho_c h'_{w,l-1}) - p_{well,l})$$

$$- \pi r_{pw}^2{}_{well,l+1} k_{well,l+1} \frac{k_{rb\,well,l+1}}{\mu_b B_{l+1}} (p_{well,l} - \rho_b g B_{l+1}$$

$$- gH_l(\rho_b - \rho_b h'_{w,l} + \rho_c h'_{w,l}) - p_{well,l+1}) \Big\} + c_b W(u_{w,l,well}) \bigg] \tag{33}$$

The SF method reduces the problem's complexity in several ways. First, unlike the CF method, it becomes unnecessary to determine effective phase dependent parameters such as density, relative conductivity, and viscosity. We do not have to assume a method for determining these effective parameters. In the SF method, the CO$_2$ portion of Equation (32) uses CO$_2$'s relative conductivity and viscosity while the brine portion of Equation (32) uses the relative conductivity and viscosity of brine.

In addition, it simplifies the complexity of calculating Green's functions from Equation (1). Using the CF method, it quickly becomes difficult to choose between using volumetric CO$_2$ fluxes, Q_c, and total volumetric flow rates, Q_{well}, when determining discretization breaks. The SF method always uses CO$_2$ volumetric flow rates when calculating Green's function values and brine volumetric flow rates when calculating Well function values.

Figure 9 shows the radial fluid pressure distribution for a single well injecting CO$_2$ or brine into a confined aquifer for 2500 days. In both cases, either method produces exactly the same fluid pressure distributions. Both methods use (1) in the case of pure CO$_2$ flux, however, it is interesting to note that (1) I mimics (27) in the case of pure brine flux.
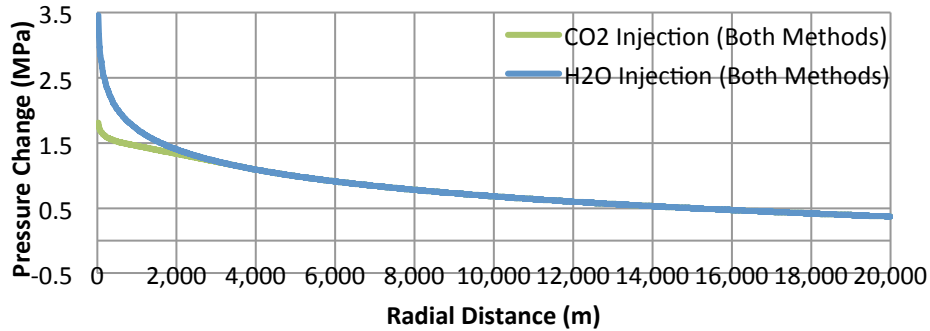
Figure 9. Aquifer pressure change vs. radial distance when individually injecting brine or CO$_2$

Figure 10 shows the radial fluid pressure distribution for a single well injecting both CO_2 and brine. Both methods simulated a mixture of 50% CO_2 and 50% brine (by volume) being injected into a confined aquifer for 2500 days. While the fluid pressure changes converged at a distance of approximately 2.5 km, pressure changes estimated using the SF method were much higher than pressure changes calculated using the CF method near the injection well. This is because if the radial distance is within the CO_2 plume the CF method assumes that the total flux behaves as CO_2 flux.
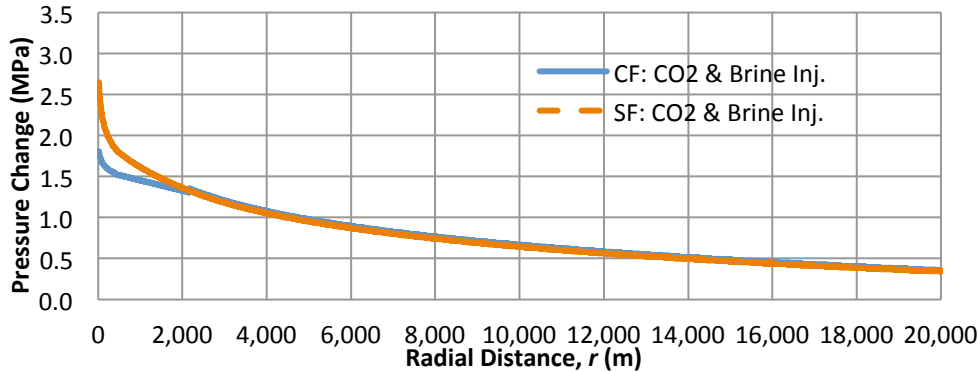
Figure 10. Aquifer pressure change vs. radial distance when simultaneously injecting both brine and **CO_2**

Figure 11 shows the CO_2 and brine leaky well flux rates verse time calculated using the CF and SF methods. Figure 12 compares fluid pressure in both layers at the leaky well over time between the CF and SF methods. Both algorithms also use the AS method.
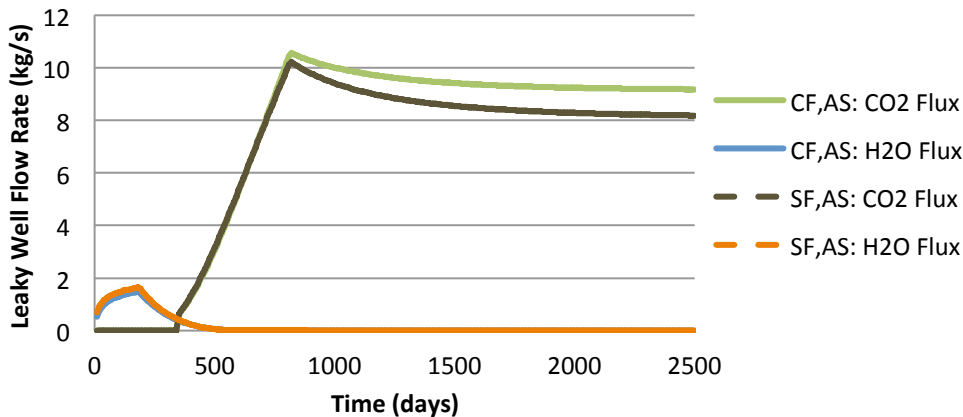
Figure 11. Leaky well flow rates vs. time

Lower CO_2 flux rates are calculated using the SF method because of a higher pressure sensitivity to fluid flux. While the SF method initially predicts greater increases in fluid pressure in the bottom layer, leaky well flow rates cause greater increases in the top layer's fluid pressure. This reduces the pressure gradient (Figure 12) resulting in less leakage. In other words, less leakage is needed to equalize the pressure differential between aquifer layers because the SF method estimates more pressure change per volumetric unit of leakage.
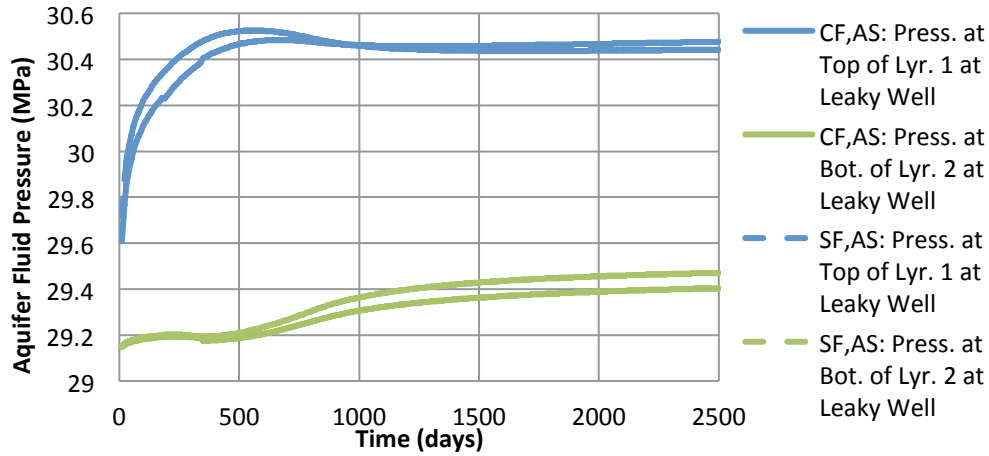
Figure 12. Aquifer fluid pressures vs. time

Conclusions

This work has led to several important observations and recommendations concerning the semi-analytical algorithm developed by Celia et. al. (2011) and Nordbotten et. al. (2009). Interestingly, the CO_2 pressure equation (1) provides exactly the same pressure distribution at the Theis equation (27) in the case of pure brine flux. Steep increases in leaky well CO_2 flux rates occur as a result of the rapidly increasing relative permeability due to increasing lower layer plume thicknesses. Also, CO_2 flux rate increases abruptly reduce when the relative permeability reaches unity.

There are two possibilities concerning the pressure offset term $F(h')$. First, when domains have relatively high aquifer permeabilities or thicknesses fundamental assumptions are violated and the algorithm is rendered unsuitable. The second possibility occurs when domains have relatively low aquifer permeabilities and thicknesses. In this case, (1)'s assumed conditions are met and $F(h')$ is negligible. A reasonable suggestion based upon this work would be to first check if $F(h')$ is negligible. If this is the case, proceed with the simulation using the semi-analytical model. Otherwise, the injection site's domain is not suitable for the semi-analytical leakage model.

Changes in fluid pressure should be calculated by multiplying Green's functions by average flow rates not end of time-step flow rates. Artificially low leaky well flow rates have been estimated when $Q_t > Q_{avg}$ and ETS method is used. In addition, aquifer fluid pressures have smoother transitions through time using the AS method. This work's results indicate that the AS method should always be used as it seems to produce more accurate flux rates and leakage values throughout the simulation duration.

Separating leaky well CO_2 and brine fluxes and applying the Theis solution to estimate pressure changes resulting from brine flow eliminating this model's need to make assumptions concerning the discontinuous nature of (1) and effective phase dependent parameters, such as density, relative conductivity.

The SF method returns lower CO_2 flux rates than the CF method. The reason for this is less flux is needed to equalize the pressure differential between aquifer layers because the SF method estimates more pressure change per volumetric unit of leakage.

This method needs numerical modeling testing to verify fluid pressure responses however it shows promise in providing a more accurate solution.

References

Celia, M. A., J. M. Nordbotten, B. Court, M. Dobossy, S. Bachu (2011). Field-scale application of a semi-analytical model for estimation of CO_2 and brine leakage along old wells, International Journal of Greenhouse Gas Control, 5: 257-269.

Nordbotten, J. M., D. Kavetski, M. A. Celia and S. Bachu (2009). Model for CO_2 leakage Including Multiple Geological Layers and Multiple Leaky Wells. Environmental Science & Technology, 43: 743-749.

Nordbotten, J.M. and M.A. Celia (2006). Similarity solutions for fluid injection into confined aquifers. J. Fluid Mech., 561: 307-327.

Nordbotten, J.M.; M.A. Celia and S. Bachu (2005a). Injection and Storage of CO_2 in Deep Saline Aquifers: Analytical Solution for CO_2 Plume Evolution During Injection. Transp Porous Med, 58: 339-360.\

Nordbotten, J.M.; M.A. Celia and S. Bachu (2005b). Semianalytical Solution for CO_2 Leakage through an Abandoned Well. Environ. Sci. Technol., 39: 602-611.

Nordbotten, J.M.; M.A. Celia and S. Bachu. (2004). Analytical solutions for leakage rates through abandoned wells. Water Resources Research, 40. W04204, doi: 10.1029/2003WR002997.